JAERI-M
82-156

SURFACE MATERIALS CONSIDERATIONS FOR FUSION REACTORS

November 1982

Kazuho SONE, Masaki MAENO, Shin YAMAMOTO
Hidewo OHTSUKA and Tetsuya ABE

日本原子力研究所
Japan Atomic Energy Research Institute

JAERI-Mレポートは，日本原子力研究所が不定期に公刊している研究報告書です。
入手の問合わせは，日本原子力研究所技術情報部情報資料課（〒319-11茨城県那珂郡東海村）あて，お申しこしください。なお，このほかに財団法人原子力弘済会資料センター（〒319-11 茨城県那珂郡東海村日本原子力研究所内）で複写による実費頒布をおこなっております。

JAERI-M reports are issued irregularly.
Inquiries about availability of the reports should be addressed to Information Section Division of Technical Information, Japan Atomic Energy Research Institute, Tokai-mura, Naka-gun Ibaraki-ken 319-11, Japan.

編集兼発行　日本原子力研究所
印　　刷　(株)原子力資料サービス

JAERI-M 82-156

Surface Materials Considerations for Fusion Reactors

Kazuho SONE, Masaki MAENO, Shin YAMAMOTO
Hidewo OHTSUKA and Tetsuya ABE+

Division of Thermonuclear Fusion Research,
Tokai Research Establishment, JAERI

(Received October 30, 1982)

Surface materials considerations have been made to support the Impurity Control and First Wall Engineering task in the INTOR. They focussed on low-Z material candidates including C(graphite), SiC and TiC. Properties considered are listed in the following:

1) Physical Sputtering
2) Chemical Sputtering
3) Arcing
4) H/He Retention/Release
5) Redeposited Materials Characteristics

Keywords: Fusion Reactors, Surface Materials, Impurity Control, Fisrt Wall Engineering, Physical Sputtering, Chemical Sputtering, Arcing, H/He Retention/Release, Redeposited Materials Characteristics, Low-Z Materials, Graphite, SiC, TiC

+ Division of Large Tokamak Development, Tokai Research Establishment, JAERI

JAERI－M 82－156

核融合炉の表面材料に関する考察

日本原子力研究所東海研究所核融合研究部
曽根　和穂・前野　勝樹・山本　　新
大塚　英男・阿部　哲也+

（1982年10月30日受理）

ＩＮＴＯＲの不純物制御および第一壁工学を支援する立場から核融合炉の表面材料に関する考察を行った。ここでは主としてＣ（黒鉛），SiC，TiCなどの低原子番号材料について述べる。考察の対象としている諸現象・性質は以下の通りである。

- 物理スパッタリング
- 化学スパッタリング
- アーキング
- 水素／ヘリウムの捕捉／再放出
- 再付着物質の性質

+ 大型トカマク開発部

CONTENTS

目　　次

1. Introduction

At INTOR Phase IIA Session V, several low-Z materials such as C(graphite), Be, BeO and SiC have been discussed as the key surface material candidates of the limiter/divertor plate, since medium- and high-Z materials should be ruled out because of self-sputtering problems in the medium-T limiter design of INTOR, where an ion temperature of 675 eV is considered. There are both advantages and disadvantages in these materials if we take account of severe conditions of irradiation of surface materials with energetic particles and high heat fluxes. Here we will discuss the following properties of these materials and TiC: 1) physical sputtering, 2) chemical sputtering, 3) arcing, 4) H/He retention/release, 5) redeposited materials characteristics. The reason why TiC is included here is due to the fact that extensive research and development for this material have recently been made in JAERI for the purpose of impurity control by low-Z coating of the limiters and the walls of JT-60, which is often very useful to discuss the other materials.

2. Physical Sputtering

Physical sputtering yield data by light ions (i.e. H^+, D^+, He^+) bombardment in the energy range below 10 keV at room temperature have been extensively compiled by Roth, Bohdansky and Ottenberger [1] in 1979. The data for the materials Be, C, SiC and TiC can be found there all having values of 0.01 to 0.03 atoms/ion in the energy range of interest 300 eV to 3 keV. Very little data are available for self-ion sputtering yield, but these can be calculated from theoretical prediction [2], which has succeeded in explaining heavy inert gas ion sputtering. Here we confine ourselves to some problems which are characteristic for compound low-Z materials like SiC and TiC at present.

It is predicted from a random collision cascade theory [3] that the ligher element C atom tends to suffer preferential ejection, although the effect is less pronounced than that caused by different surface potential. Silicon carbide coatings with various different atomic fractions of Si and C have been bombarded with a 3 keV H_3^+ ion beam at temperatures around 500°C [4]. The sputtering yield in stoichiometric samples (i.e. Si/C = 1) at 500°C is 1.15×10^{-2} atoms/H^+. As the

1. Introduction

At INTOR Phase IIA Session V, several low-Z materials such as C(graphite), Be, BeO and SiC have been discussed as the key surface material candidates of the limiter/divertor plate, since medium- and high-Z materials should be ruled out because of self-sputtering problems in the medium-T limiter design of INTOR, where an ion temperature of 675 eV is considered. There are both advantages and disadvantages in these materials if we take account of severe conditions of irradiation of surface materials with energetic particles and high heat fluxes. Here we will discuss the following properties of these materials and TiC: 1) physical sputtering, 2) chemical sputtering, 3) arcing, 4) H/He retention/release, 5) redeposited materials characteristics. The reason why TiC is included here is due to the fact that extensive research and development for this material have recently been made in JAERI for the purpose of impurity control by low-Z coating of the limiters and the walls of JT-60, which is often very useful to discuss the other materials.

2. Physical Sputtering

Physical sputtering yield data by light ions (i.e. H^+, D^+, He^+) bombardment in the energy range below 10 keV at room temperature have been extensively compiled by Roth, Bohdansky and Ottenberger [1] in 1979. The data for the materials Be, C, SiC and TiC can be found there all having values of 0.01 to 0.03 atoms/ion in the energy range of interest 300 eV to 3 keV. Very little data are available for self-ion sputtering yield, but these can be calculated from theoretical prediction [2], which has succeeded in explaining heavy inert gas ion sputtering. Here we confine ourselves to some problems which are characteristic for compound low-Z materials like SiC and TiC at present.

It is predicted from a random collision cascade theory [3] that the ligher element C atom tends to suffer preferential ejection, although the effect is less pronounced than that caused by different surface potential. Silicon carbide coatings with various different atomic fractions of Si and C have been bombarded with a 3 keV H_3^+ ion beam at temperatures around 500°C [4]. The sputtering yield in stoichiometric samples (i.e. Si/C = 1) at 500°C is 1.15×10^{-2} atoms/H^+. As the

stoichiometry deviates from this point, the sputtering yield has larger values (Fig. 1). The temperature dependence of the sputtering yield in stoichiometric samples is negligible below 600°C from the comparison with a room temperature value [5]. By Auger electron spectroscopy (AES), carbon exists on the surface in the form of carbide in stoichiometric SiC before and after the bombardment, while it exists in the form of graphite in C-rich samples, which suggests that the bound state of carbon in the form of carbide should correspond to the low sputtering yield in stoichiometric SiC coatings. The stoichiometry changes due to hydrogen bombardment are observed by the AES and electron probe X-ray microanalysis, where the carbon population increases in stoichiometric SiC, while it decreases in C-rich samples.

These results are closely connected with surface segregation of C atoms by heating the sample up to ∿1000°C [6, 7], or with preferential evaporation of Si atoms at temperatures below 2000°C [8]. The surface segregation of C atoms by heating is observed also in B_4C [7]. The C atoms segregated to the surface will experience physical sputtering when the surface is bombarded with energetic particles, although it will experience chemical sputtering as well if the particles are hydrogens. In fact, physical sputtering reduces the carbon population at the surface by an Ar^+ ion beam (3 keV, 8 μA) in SiC and B_4C. On the other hand, TiC surface is very stable against the heating and no surface segregation is observed even at 1000°C. However, with the Ar^+ ion bombardment carbon atoms segregated slightly to the surface with the atomic ratio Ti/C of 0.87. A similar phenomenon has been assumed in methane formation in TiC by low energy proton bombardment at temperature below 700°C [9], where it is called 'enhanced diffusion' by ion bombardment.

3. Chemical Sputtering

Chemical sputtering means material removal through chemical reactions with reactive gaseous speciés occurring at the surface. For low-Z materials like C, SiC and TiC, methane formation is mostly investigated which occurs in the temperature range below 900°C.

Methane formation during proton bombardment of different forms of carbon materials (i.e. pyrolytic graphite, isotropic carbon and glassy carbon) in the proton energy range between 100 eV and 6 keV has been

stoichiometry deviates from this point, the sputtering yield has larger values (Fig. 1). The temperature dependence of the sputtering yield in stoichiometric samples is negligible below 600°C from the comparison with a room temperature value [5]. By Auger electron spectroscopy (AES), carbon exists on the surface in the form of carbide in stoichiometric SiC before and after the bombardment, while it exists in the form of graphite in C-rich samples, which suggests that the bound state of carbon in the form of carbide should correspond to the low sputtering yield in stoichiometric SiC coatings. The stoichiometry changes due to hydrogen bombardment are observed by the AES and electron probe X-ray microanalysis, where the carbon population increases in stoichiometric SiC, while it decreases in C-rich samples.

These results are closely connected with surface segregation of C atoms by heating the sample up to ∿1000°C [6, 7], or with preferential evaporation of Si atoms at temperatures below 2000°C [8]. The surface segregation of C atoms by heating is observed also in B_4C [7]. The C atoms segregated to the surface will experience physical sputtering when the surface is bombarded with energetic particles, although it will experience chemical sputtering as well if the particles are hydrogens. In fact, physical sputtering reduces the carbon population at the surface by an Ar^+ ion beam (3 keV, 8 μA) in SiC and B_4C. On the other hand, TiC surface is very stable against the heating and no surface segregation is observed even at 1000°C. However, with the Ar^+ ion bombardment carbon atoms segregated slightly to the surface with the atomic ratio Ti/C of 0.87. A similar phenomenon has been assumed in methane formation in TiC by low energy proton bombardment at temperature below 700°C [9], where it is called 'enhanced diffusion' by ion bombardment.

3. Chemical Sputtering

Chemical sputtering means material removal through chemical reactions with reactive gaseous speciés occurring at the surface. For low-Z materials like C, SiC and TiC, methane formation is mostly investigated which occurs in the temperature range below 900°C.

Methane formation during proton bombardment of different forms of carbon materials (i.e. pyrolytic graphite, isotropic carbon and glassy carbon) in the proton energy range between 100 eV and 6 keV has been

investigated, from which we obtain a conclusion that energy and temperature dependences of methane formation yield per incident H^+ are not affected by different forms of the carbon materials [10]. Temperature dependence of methane formation can be explained by the model proposed by Erents al. [11, 12]. According to the model, the rate of formation of methane γ is given by

$$\gamma = \frac{AJ_o \exp(-Q_1/RT)}{J_o\sigma + \tau^{-1}} \quad , \qquad \text{where } \tau = \tau_o \exp(Q_2/RT) \quad , \tag{1}$$

where J_o is incident ion flux, σ detrapping cross section of hydrogen atoms induced by subsequently incident ions, and $A \exp(-Q_1/RT)$ means the chemical reaction rate for the formation of methane, A being a constant. If we take account of the particle backscattering whose coefficient is denoted by B, eq.(1) can be changed into the following equation:

$$\gamma = \frac{AJ_o(1 - B) \exp(-Q_1/RT)}{J_o(1 - B)\sigma + \tau^{-1}} \quad . \tag{2}$$

The peak temperature T_m at which the methane formation rate has a maximum is given by

$$T_m = \frac{Q_2}{R} \left[\ln \frac{(Q_2/Q_1 - 1)}{J_o(1 - B)\sigma \tau_o} \right]^{-1} \quad . \tag{3}$$

Equations (2) and (3) give a good fit to the experimental data by choosing suitable values of parameters Q_1, Q_2 and τ_o [13, 14]. We can further develop the model by taking account of surface deposited energy together with the ion backscattering which are both dependent on the incident energy. The final form of γ is thus obtained [13] as

$$\gamma = A'(J_o f_D/\nu_o)^{\ell} \frac{J_o(1 - B) \exp(-Q_1^+/RT)}{J_o(1 - B)\sigma + \tau^{-1}} \quad , \quad \frac{1}{2} \le \ell \le 1 \tag{4}$$

where f_D is the recoil energy density at the surface, A', ν_o and Q_1^+ are new constants. The final form of T_m is obtained by replacing Q_1 by Q_1^+

in eq.(3). Equation (4) predicts well the flux and energy dependences of methane formation rate if the value ℓ is chosen to be 0.75 [13] for proton incidence and 0.6 for deuteron incidence [14] (Fig. 2). There is a pronounced maximum in the vicinity of 1 keV for the methane formation yield per incident ion at any incident fluxes. The yield at a given energy increases with increasing incident flux. Thus we have to define three parameters of incident energy, incident flux and target temperature to say the value of the chemical sputtering yield. For the absolute values, see Fig. 2.

Chemical sputtering process in compound materials such as SiC and TiC is more complicated. In the case of SiC, the both elements C and Si have the strong reactivity with atomic hydrogens producing volatile methane and silane molecules, respectively. The result of the experiment in which methane produced is detected indicates that methane formation rate is decreased with increasing fluence due to depletion of C atoms in a Si-rich silicon carbide [15]. Since the variation of silicon hydride formation such as silane was not detected there simultaneously with methane formation, we cannot know the stationary concentration of Si and C atoms. From the considerations of surface segregation of C atom at high temperatures below 1000°C mentioned in the preceding section, C atoms are supplied from the bulk and they will be chemically sputtered by hydrogen bombardment. On the contrary, chemical affinity of SiH(g) formation from Si(s) + H is higher than that of CH(g) formation from C(s) + H [16]. Therefore, the idea of C atom depletion is not consistent with the above considerations on stoichiometric SiC. From the AES analysis of the bombarded surface in stoichiometric SiC, the Si atom concentration is reduced by a factor of 10 $\sim$ 25 % [4]. The result is supported by another experiment using ESCA technique [17], which clearly indicates that the chemical bond between Si and C atoms is destroyed by 4 keV hydrogen bombardment, and that the Si atoms get out of the surface whereas the C atoms remain on the surface in the form of graphite. This suggests that chemical sputtering in silicon carbide strongly depends on the sample characterisation, especially the surface composition of Si and C atoms. In the case of TiC, methane formation by H^+ bombardment has been measured in the energy range between 100 eV and 1 keV at temperatures below 700°C [9]. The yield per incident H^+ is one order of magnitude less than that of graphite and show little temperature dependence. It has a maximum around 2 keV which is similar

to that of physical sputtering yield of Ti. The dose dependence of the yield is mainly attributed to the surface concentration of C atoms different from the steady concentration which is produced by enhanced diffusion of C atoms by H^+ bombardment.

In addition to the chemical sputtering by energetic hydrogen bombardment, chemical erosion by thermal atomic hydrogens should be noted. Measurements have been made of the erosion rate of graphite by atomic hydrogen shower in the temperature range between 100°C and 900°C [18]. The result indicates that the graphite surface becomes inactive to atomic hydrogen after it is exposed to hydrogen atoms to a fluence of 10^{17} H/cm^2 at 500°C or higher. Methane production rate is drastically reduced with the run number of conditioning by atomic hydrogens, and the peak which is seen clearly disappears with the run (Fig. 3). This inactive graphite surface thus conditioned is restored again to the initial state when it is exposed to air. A phenomenon similar to the above result has been demonstrated in a carbon wall experiment in DIVA [19]. But we have to pay attention as well to the following experimental result [20]. The methane formation yield by energetic hydrogen ion (3 keV H_3^+) bombardment of the conditioned surface in vacuum by atomic hydrogens, which is expected inactive, is the same as that of the non-conditioned surface by atomic hydrogens. The reason is due to the fact that the inactive graphite surface obtained by the atomic hydrogen pre-exposure can be destroyed by the energetic ion bombardment.

It is important to look at the recent experimental results of sputtering yield of graphite for 1 keV H^+ and D^+ ions at elevated temperatures [21]. As the temperature is raised beyond 525°C (i.e. peak temperature for methane formation) the erosion rate decreases. However, above ∿1000°C erosion again increases monotonically with no apparent peak and exceeds the methane maximum value at ∿1500°C. The high erosion rates observed above ∿1000°C indicate a mechanism other than physical or chemical sputtering process, since no hydrocarbon formation such as acetylene is detected at the high temperatures. A possible explanation being considered is that carbon diffuses to the surface due to vacancy migration forming weakly bound carbon clusters which exhibit a high sputtering yield [21].

4. Arcing

Arc tracks on material surfaces have been observed in many tokamaks. It has been suggested that arcing is one of the dominant mechanisms for introducing metal impurities into tokamak plasma [22]. Recent time- and space-resolved studies of unipolar arcing have shown that arcing is related to particular plasma conditions characteristic of unstable discharge phase such as the current rise and end phases as well as during plasma disruption, and that runaway electrons produce a large potential difference between plasma and material to initiate arcing [23-25]. As for the dependence of arcing on surface material, we have found no apparent difference among various materials, for example, Mo, SiC, TiC, Be, Stainless Steel, C and Al which are used in the JFT-2 tokamak. Arc phenomenon seems to be independent of materials. Hence we restrict ourselves to discussing possibility of arcing and related surface problems in future large tokamaks. Plasma parameters related to arcing have been measured by the double probe method and the sheath electric field E has been cleared to be about 3×10^7 V/m [26]. If arcing would occur in the steady state of future large tokamaks such as INTOR, arcing will be one of the dominant mechanisms for introducing metal impurities into the plasma and surface damage will be a serious problem.

According to the sheath theory, the wall potential ϕ_w is

$$-\phi_w = \frac{T_{eb}}{2e} \{ \ell n(\frac{m_i}{m_e}) - \ell n 2\pi - 2\ell nM \} \quad , \tag{5}$$

where T_{eb} is the electron temperature in the scrape-off plasma, and m_i, m_e are ion and electron masses, M is the Mach number of the initial velocity of ion in the sheath layer [27]. Since the electric potential ϕ_i related to the thermal energy of ions is

$$\phi_i = \frac{T_{eb}}{2e} M^2 \quad , \tag{6}$$

the potential difference ϕ_s between the plasma and the wall is

$$-\phi_s = -\phi_w + \phi_i = \frac{T_{eb}}{2e} \{ \ell n(\frac{m_i}{m_e}) - \ell n 2\pi - 2\ell nM + M^2 \} \quad . \tag{7}$$

In this case M is unity and $m_i = 1840\, A m_e$ (A is the atomic number).

Therefore, the potential difference ϕ_s between the plasma and the wall is

$$-\phi_s = 3.3 \frac{T_{eb}}{e} (1 + 0.15 \ell nA) \quad . \tag{8}$$

The sheath layer λ_s is

$$\lambda_s = 3\lambda_D \quad , \tag{9}$$

where λ_D is the Debye shielding length and given as

$$\lambda_D = 7.45 \sqrt{\frac{T_{eb}}{n_{eb}}} \quad , \tag{10}$$

where n_{eb} is the electron density in the scrape-off plasma. Thus, the electric field E_s between the plasma and the wall is given by

$$E_s = 1.5 \times 10^{-4} \frac{T_{eb}}{e} \sqrt{\frac{n_{eb}}{T_{eb}}} \quad . \tag{11}$$

The field E_s is a function of T_{eb} and n_{eb}. Solid curves in Fig. 4 show the dependence of E_s on T_{eb} for a hydrogen plasma as a parameter of n_{eb}.

The heat flux density q (W/cm^2) towards an electically insulated conducting plate in a plasma is written as follows

$$q = \gamma I_s T_{eb} \quad , \tag{12}$$

where I_s (A/cm^2) is the ion saturation current density, $\gamma = 7.8$ for hydrogen plasma of $T_{eb} = T_{ib}$, T_{ib} being the proton temperature in the scrape-off plasma [28]. The current I_s is given as follows

$$I_s = \frac{n_{eb}}{2} \sqrt{\frac{T_{eb}}{M_i}} \quad , \tag{13}$$

where M_i is the ion mass. Dashed lines in Fig. 4 show the dependence of q on T_{eb} and n_{eb} for a hydrogen plasma.

Operation conditions in future large tokamaks will be limited by the heat load on the first wall. This means that if the temperature T_{eb} will be higher, the density must be kept lower as to reduce the

heat flux density. The maximum permissible heat flux density to the first wall is considered to be about 100 W/cm^2. On the other hand, the electric field between the plasma and the wall is below 2×10^6 V/m in the above mentioned plasma parameters (Fig. 4). This value is about one-tenth of the electric field to initiate monopolar arcing.

On the basis of these facts, it is considered that monopolar arcing will scarecely occur in the steady state of future large tokamaks.

5. H/He Retention/Release

Hydrogen retention/release is closely connected with possibility of recycling rate control at the wall when neutral beam injection heating is used in large tokamaks. The idea and technique are also available for the tritium inventory evaluation and permeation problem. Here we show an example of the recycling rate calculation applied to JT-60 [29]. Such calculation is particularly useful, since it is not easy to simulate synthetically by accelerator experiments hydrogen recycling behaviours (e.g. backscattering, trapping, detrapping, permeation etc.) at wall surfaces of tokamaks by taking account of their operation conditions.

The calculation has been made essentially on the basis of hydrogen diffusion from the bulk of the wall, which can generally be given by the differential equation:

$$\frac{\partial c(x,\ t)}{\partial t} = D\ \frac{\partial^2 c}{\partial x^2} + G(x) \quad , \tag{14}$$

where D : diffusion coefficient of hydrogen in the wall,

$c(x, t)$: concentration of hydrogen atoms at depth x and time t,

$G(x)$: source term of hydrogen atoms at x.

Thus the re-emission rate is obtained from $-D\ \partial c/\partial x\big|_{x=0}$ + backscattering + excess over saturation concentration. As a first approximation, the boundary condition is given as $c(0, t) = 0$, which is justified in endothermic materials [30]. The source term for random incidence used here is

$$G(x) = \int_0^{\pi/2} d\theta \int_0^{\infty} dE\ \sin 2\theta\ f(E)\ \rho_o(x, E, \theta) \quad . \tag{15}$$

heat flux density. The maximum permissible heat flux density to the first wall is considered to be about 100 W/cm^2. On the other hand, the electric field between the plasma and the wall is below 2×10^6 V/m in the above mentioned plasma parameters (Fig. 4). This value is about one-tenth of the electric field to initiate monopolar arcing.

On the basis of these facts, it is considered that monopolar arcing will scarecely occur in the steady state of future large tokamaks.

5. H/He Retention/Release

Hydrogen retention/release is closely connected with possibility of recycling rate control at the wall when neutral beam injection heating is used in large tokamaks. The idea and technique are also available for the tritium inventory evaluation and permeation problem. Here we show an example of the recycling rate calculation applied to JT-60 [29]. Such calculation is particularly useful, since it is not easy to simulate synthetically by accelerator experiments hydrogen recycling behaviours (e.g. backscattering, trapping, detrapping, permeation etc.) at wall surfaces of tokamaks by taking account of their operation conditions.

The calculation has been made essentially on the basis of hydrogen diffusion from the bulk of the wall, which can generally be given by the differential equation:

$$\frac{\partial c(x,\ t)}{\partial t} = D\ \frac{\partial^2 c}{\partial x^2} + G(x) \quad , \tag{14}$$

where D : diffusion coefficient of hydrogen in the wall,

$c(x, t)$: concentration of hydrogen atoms at depth x and time t,

$G(x)$: source term of hydrogen atoms at x.

Thus the re-emission rate is obtained from $-D\ \partial c/\partial x\big|_{x=0}$ + backscattering + excess over saturation concentration. As a first approximation, the boundary condition is given as $c(0, t) = 0$, which is justified in endothermic materials [30]. The source term for random incidence used here is

$$G(x) = \int_0^{\pi/2} d\theta \int_0^{\infty} dE\ \sin 2\theta\ f(E)\ \rho_o(x, E, \theta) \quad . \tag{15}$$

$$\rho_o(x, E, \theta) = \sqrt{\frac{2}{\pi}} \frac{J_o \{1 - B(E, \theta)\}}{\Delta R_p [1 + \mathrm{erf}(\varepsilon_o)]} \cdot \exp\{-\frac{(x - R_p \cos\theta)^2}{2\Delta R_p^2}\} ,$$

$$\varepsilon_o = \frac{R_p \cos\theta}{\sqrt{2}\, \Delta R_p}$$

where θ : angle of incidence with respect to the surface normal,
J_o : incident flux of hydrogen atoms to the wall,
R_p : projected range of hydrogen atoms of energy E,
ΔR_p : range straggling of hydrogen atoms of energy E,
$B(E, \theta)$: backscattering coefficient of hydrogen atoms incident with the angle θ, and energy E.

An example of the calculated results for three different wall materials Inconel, molybdenum and TiC is shown with the shot number of a pulse operation cycle of 5 sec discharge and 10 min interruption (Fig. 5). The calculated results shown in Fig. 5 is for the case of monoenergetic (E = 1 keV) particle incidence with a flux J_o of 1×10^{16} H/cm^2 sec. The wall temperature rise with shot number is assumed to be 13 °C/shot (initial temperature 60°C), which is the slowest case assumed. The code HRECYCLE is applicable to any incident energy distributions given, for instance, the maxwellian energy distribution (Fig. 6). In such calculations including hydrogen retention and permeation, there are two main problems. One is the ambiguity of the diffusion coefficient including radiation damage effect and the other is how to give the boundary condition in eq.(15) including surface recombination of atomic hydrogens diffusing from the bulk. Under more realistic conditions, the wall surface is bombarded with energetic particles, which produces dense trapping sites in the surfac layers which reduces the diffusion coefficient to about two orders of magnitudes lower in Ni [31]. The radiation damage effect on retention/release has been observed in carbon [32] which is very similar to the molybdenum case [33]. Since the actual wall surface will become rough and porous by redeposition/contamination, a more realistic recombination coefficient will be necessary, which could change considerably the boundary condition of eq.(14).

Surface roughness has a strong effect on helium gas release behaviour as well as surface erosion, when various forms of carbon and TiC are bombarded with 200 keV He^+ ions [34, 35]. The fluence at which the re-emission rate begins to increase becomes higher in a smooth surface

than in rough one. With increasing fluence re-emission burst occurs frequently in the smooth surface, which does not occur in the rough one. The frequent re-emission burst is due to successive exfoliation of the surface layer which does not take place in the rough surface.

6. Redeposited Materials Characteristics

The first wall materials are eroded by sputtering, blistering and evaporation processes during plasma operation. The eroded materials will redeposit on other parts of the first wall [36]. However, little is known at present about the nature of redeposited materials in the field of plasma-wall interactions. This redeposition phenomenon is also an important problem in the field of thin solid film technology in order to control deposited film qualities. We consider here the redeposition problem of the first wall materials in relation to the technology.

1) The redeposition process may be different between the case when the first wall materials are made of compounds/alloys and the case when they are single element materials. In the case of compounds/alloys such as SiC and stainless steel, there is a possibility of variation in the surface composition of the first wall materials because of preferential sputtering/evaporation for a certain element [37, 38]. Therefore, the composition of redeposited materials might be different from that of the first wall material itself. This does not take place for single element material such as C and Be.

2) It is important to increase adhesiveness of the redeposited particles to the wall surface. If it is weak they will easily leave the wall surface and enter the plasma as impurities.

Acknowledgements

The authors would like to thank Drs. T. Hiraoka and Y. Murakami for their kind suggestions of initiating the present work. They also acknowledge Drs. M. Tanaka and Y. Obata for their continuous encouragement.

than in rough one. With increasing fluence re-emission burst occurs frequently in the smooth surface, which does not occur in the rough one. The frequent re-emission burst is due to successive exfoliation of the surface layer which does not take place in the rough surface.

6. Redeposited Materials Characteristics

The first wall materials are eroded by sputtering, blistering and evaporation processes during plasma operation. The eroded materials will redeposit on other parts of the first wall [36]. However, little is known at present about the nature of redeposited materials in the field of plasma-wall interactions. This redeposition phenomenon is also an important problem in the field of thin solid film technology in order to control deposited film qualities. We consider here the redeposition problem of the first wall materials in relation to the technology.

1) The redeposition process may be different between the case when the first wall materials are made of compounds/alloys and the case when they are single element materials. In the case of compounds/alloys such as SiC and stainless steel, there is a possibility of variation in the surface composition of the first wall materials because of preferential sputtering/evaporation for a certain element [37, 38]. Therefore, the composition of redeposited materials might be different from that of the first wall material itself. This does not take place for single element material such as C and Be.

2) It is important to increase adhesiveness of the redeposited particles to the wall surface. If it is weak they will easily leave the wall surface and enter the plasma as impurities.

Acknowledgements

The authors would like to thank Drs. T. Hiraoka and Y. Murakami for their kind suggestions of initiating the present work. They also acknowledge Drs. M. Tanaka and Y. Obata for their continuous encouragement.

than in rough one. With increasing fluence re-emission burst occurs frequently in the smooth surface, which does not occur in the rough one. The frequent re-emission burst is due to successive exfoliation of the surface layer which does not take place in the rough surface.

6. Redeposited Materials Characteristics

The first wall materials are eroded by sputtering, blistering and evaporation processes during plasma operation. The eroded materials will redeposit on other parts of the first wall [36]. However, little is known at present about the nature of redeposited materials in the field of plasma-wall interactions. This redeposition phenomenon is also an important problem in the field of thin solid film technology in order to control deposited film qualities. We consider here the redeposition problem of the first wall materials in relation to the technology.

1) The redeposition process may be different between the case when the first wall materials are made of compounds/alloys and the case when they are single element materials. In the case of compounds/alloys such as SiC and stainless steel, there is a possibility of variation in the surface composition of the first wall materials because of preferential sputtering/evaporation for a certain element [37, 38]. Therefore, the composition of redeposited materials might be different from that of the first wall material itself. This does not take place for single element material such as C and Be.

2) It is important to increase adhesiveness of the redeposited particles to the wall surface. If it is weak they will easily leave the wall surface and enter the plasma as impurities.

Acknowledgements

The authors would like to thank Drs. T. Hiraoka and Y. Murakami for their kind suggestions of initiating the present work. They also acknowledge Drs. M. Tanaka and Y. Obata for their continuous encouragement.

References

[1] J. Roth, J. Bohdansky and W. Ottenberger, Max-Planck-Institut für Plasmaphysik Report IPP 9/26 (1979).

[2] P. Sigmund, Phys. Rev. 184 (1969) 383.

[3] P. Sigmund, in Sputtering by Particle Bombardment, vol. I, ed. R. Behrisch (Springer Verlag, 1981), p.9.

[4] K. Sone, M. Saidoh, K. Nakamura, R. Yamada, Y. Murakami, T. Shikama, M. Fukutomi, K. Kitajima and M. Okada, J. Nucl. Mater., 98 (1981) 270.

[5] J. Bohdansky, H.L. Bay and W. Ottenberger, ibid, 76 & 77 (1978) 163.

[6] M. Mohri, K. Watanabe, T. Yamashina, H. Doi and K. Hayakawa, ibid, 85 & 86 (1979) 1185.

[7] S. Fukuda, S. Kato, K. Mohri and T. Yamashina, Proc. 5th Intern. Conf. on plasma-Surface Interactions in Controlled Fusion Devices, 1982, Gatlinburg, U.S.A.

[8] J. Drowart and G. De Maria, Proc. Conf. on Silicon Carbide, 1959, Boston (Pergamon Press, Oxford, 1960), p. 16.

[9] R. Yamada, K. Nakamura and M. Saidoh, Proc. 5th Intern. Conf. on Plasma-Surface Interactions in Controlled Fusion Devices, 1982, Gatlinburg, U.S.A.

[10] R. Yamada, K. Nakamura, K. Sone and M. Saidoh, J. Nucl. Mater., 95 (1980) 278.

[11] S.K. Erents, C.M. Braganza and G.M. McCracken, ibid, 63 (1976) 399.

[12] C.M. Braganza, S.K. Erents and G.M. McCracken, ibid, 75 (1978) 220.

[13] R. Yamada and K. Sone (to be published).

[14] K. Sone (to be published).

[15] C. Braganza, G.M. McCracken and S.K. Erents, Proc. Intern. Symp. on Plasma Wall Interaction (Pergamon Press, Oxford, 1977), p.257.

[16] JANAF Thermonuclear Tables, 2nd ed., D.R. Stull and H. Prophet, NSRDS-NBS 37 (1971).

[17] Y. Gotoh, private communication.

[18] T. Abe, K. Obara and Y. Murakami, J. Nucl. Mater., 91 (1980) 223.

[19] S. Sengoku, et al., ibid, 93 & 94 (1980) 178.

[20] R. Yamada, K. Nakamura and M. Saidoh, ibid, 98 (1981) 167.

[21] J. Roth, J. Bohdansky and K.L. Wilson, Proc. 5th Intern. Conf. on Plasma-Surface Interactions in Controlled Fusion Devices, 1982, Gatlinburg, U.S.A.

[22] G.M. McCracken and D.H.J. Goodall, Nucl. Fusion, 18 (1978) 537.

[23] S. Yamamoto, Y. Shimomura, K. Ohasa, H. Kimura, S. Sengoku, K. Odajima, T. Matsuda, H. Matsumoto, H. Ohtsuka and H. Maeda, J. Phys. Soc. Jpn., 48 (1980) 1053.

[24] M. Maeno, H. Ohtsuka, S. Yamamoto, T. Yamamoto, N. Suzuki, N. Fujisawa and N. Ogiwara, Nucl. Fusion, 20 (1980) 1415.

[25] H. Ohtsuka, N. Ogiwara and M. Maeno, J. Nucl. Mater., 93 & 94 (1980) 161.

[26] H. Ohtsuka, M. Maeno, N. Suzuki, S. Konoshima, S. Yamamoto and N. Ogiwara, Nucl..Fusion, 22 (1982) 823.

[27] T. Kawamura, Kakuyugo Kenkyu Supplement, 13 (1981) 103 (in Japanese).

[28] R.H. Lovberg, Plasma Diagnostic Technique, eds. R.H Huddlestone and S.L. Leonard (Academic Press, New York, 1965) Ch. 3.

[29] K. Sone, R. Yamada and Y. Murakami (to be published in Japan Atomic Energy Research Institute Report).

[30] M.I. Baskes, J. Nucl. Mater., 29 (1980) 318.

[31] K. Erents and G.M. McCracken, Radiat. Effects, 3 (1980) 123.

[32] K. Sone and G.M. McCracken, Proc. 5th Intern. Conf. on Plasma-Surface Interactions in Controlled Fusion Devices, 1982, Gatlinburg, U.S.A.

[33] G.M. McCracken and S.K. Erents, in Application of Ion Beams to Metals, eds. S.T. Picraux et al. (Plenum Press, New York, 1974), p.585.

[34] M. Saidoh, R. Yamada and K. Nakamura, J. Nucl. Mater., 102 (1981) 97.

[35] M. Saidoh, R. Yamada and K. Nakamura, Proc. 5th Intern. Conf. Plasma-Surface Interactions in Controlled Fusion Devices, 1982, Gatlinburg, U.S.A.

[36] J.N. Smith, Jr., C.H. Meyer, Jr. and J.S. DeGrassie, J. Vac. Sci. Technol., 20 (1982) 1279.

[37] M. Mohri, K. Watanabe and T. Yamashina, J. Nucl. Mater. 71 (1978) 7.

[38] M. Yabumoto, K. Watanabe and T. Yamashina, Surface Sci., 77 (1978) 615.

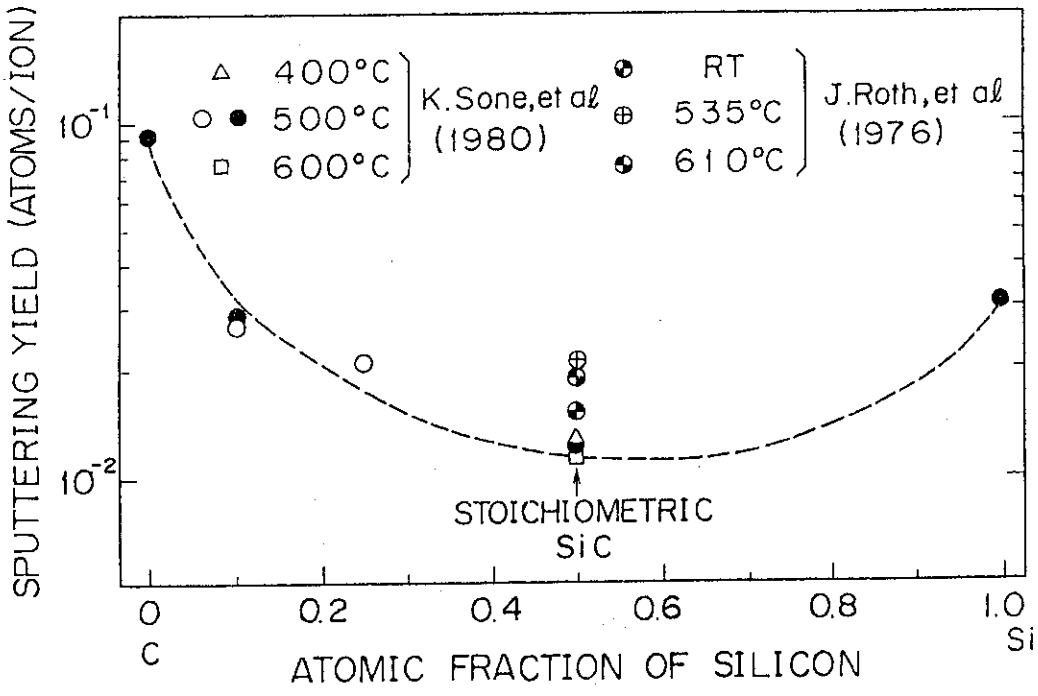

Fig. 1 Sputtering yield of silicon carbide (atoms/H^+) for a 3 keV H_3^+ beam as a function of the atomic fraction of silicon. RT denotes room temperature. RS and SS mean rough surface and smooth surface, respectively [4].

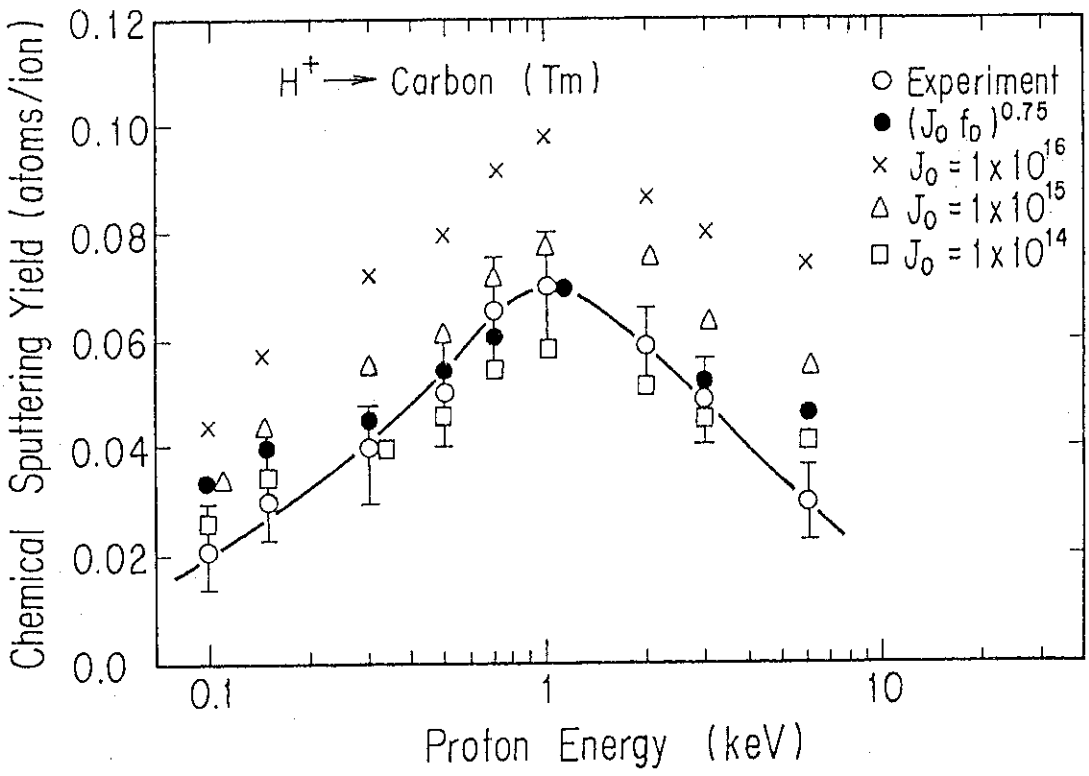

Fig. 2 Flux and energy dependences of the calculated chemical sputtering yield obtained using eq.(4) with $\ell = 0.75$. The target temperature is chosen as the peak temperature T_m given by eq.(3), and the flux of protons J_o ranges from 1×10^{14} to 1×10^{16} H/cm^{2}sec. Full circles show the calculated yields at T_m using experimental values of J_o in units of 10^{14} H/cm^{2}sec, which are 5.8, 6.0, 2.1, 2.4, 3.0, 4.4, 4.9, and 6.6 in order from the lower energy side [13].

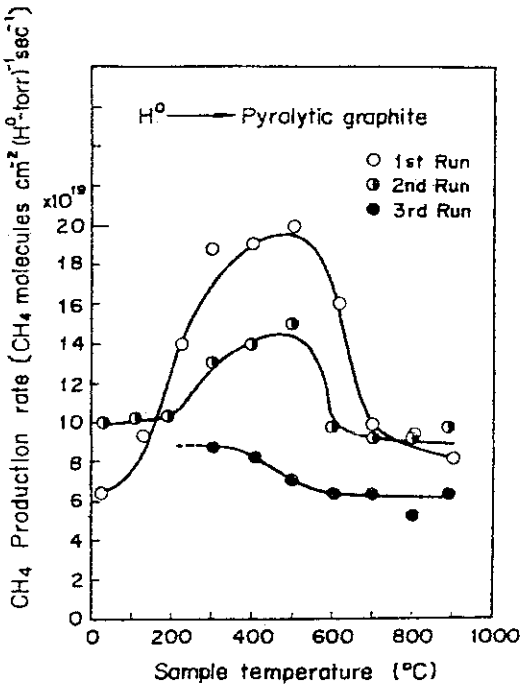

Fig. 3 Measured methane formation rates in pyrolytic graphite as a function of the sample temperature for three successive runs [18].

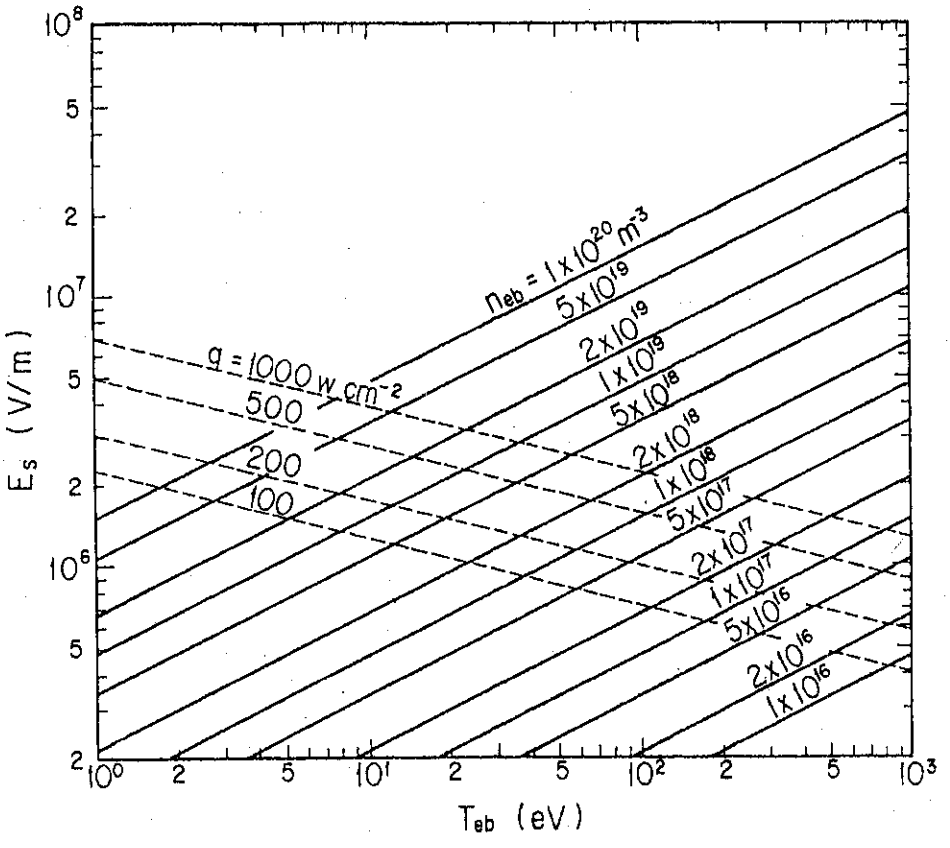

Fig. 4 Dependence of the electric field E_s between the plasma and the wall on the electron temperature T_{eb} as a parameter of the electron density n_{eb} in the scrape-off plasma (solid lines), and the dependence of the heat flux density q and T_{eb} and n_{eb} (dashed lines).

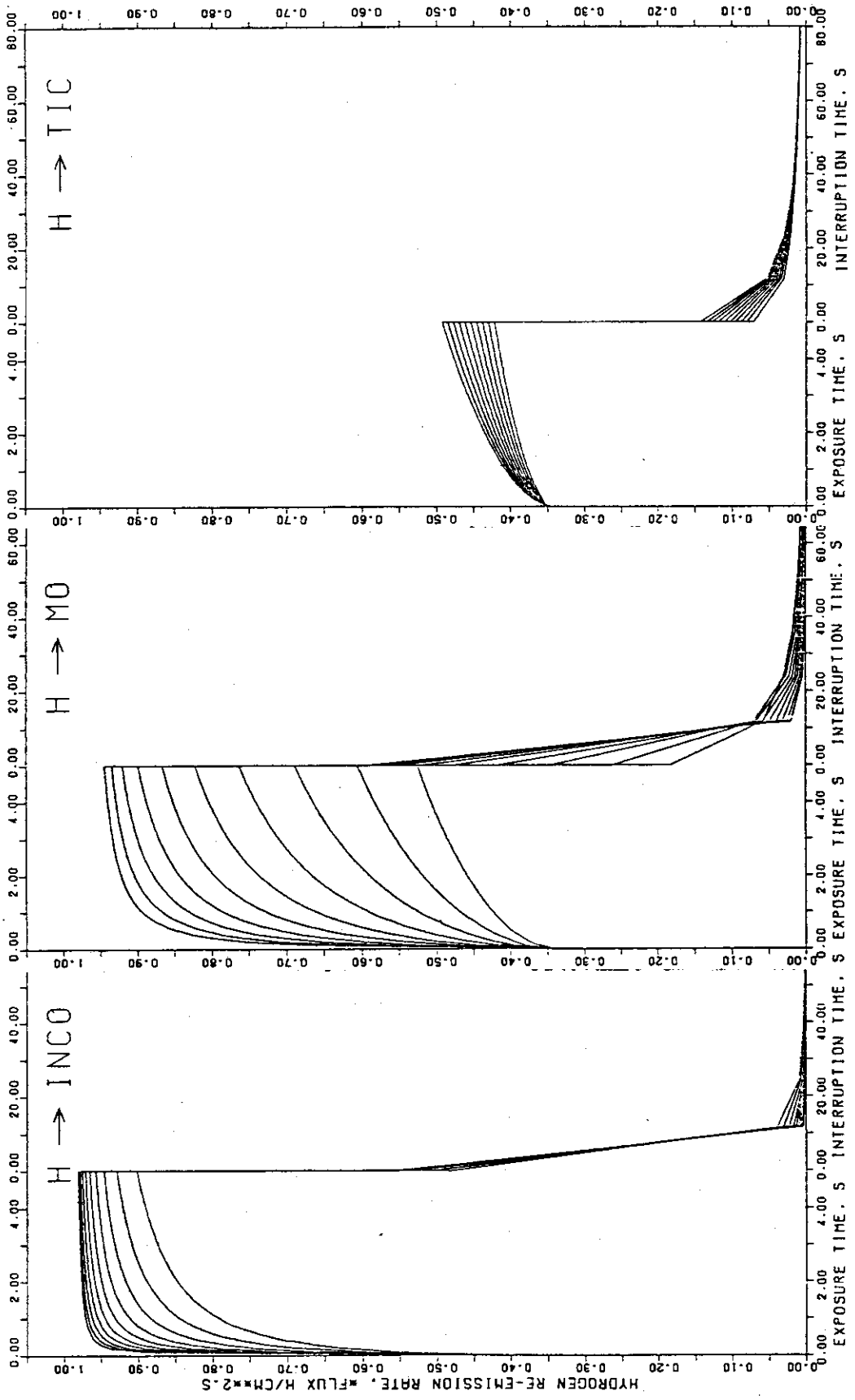

Fig. 5 Variation of recycling rate of hydrogen with shot number (up to the 10th shot) as a function of time in Inconel, molybdenum and TiC. Incident flux: $J_o = 1\times10^{16}$ H/cm^{2}sec. Incident energy: E = 1 keV. Operation schedule of one shot: 5 sec discharge and 10 min interruption [29].

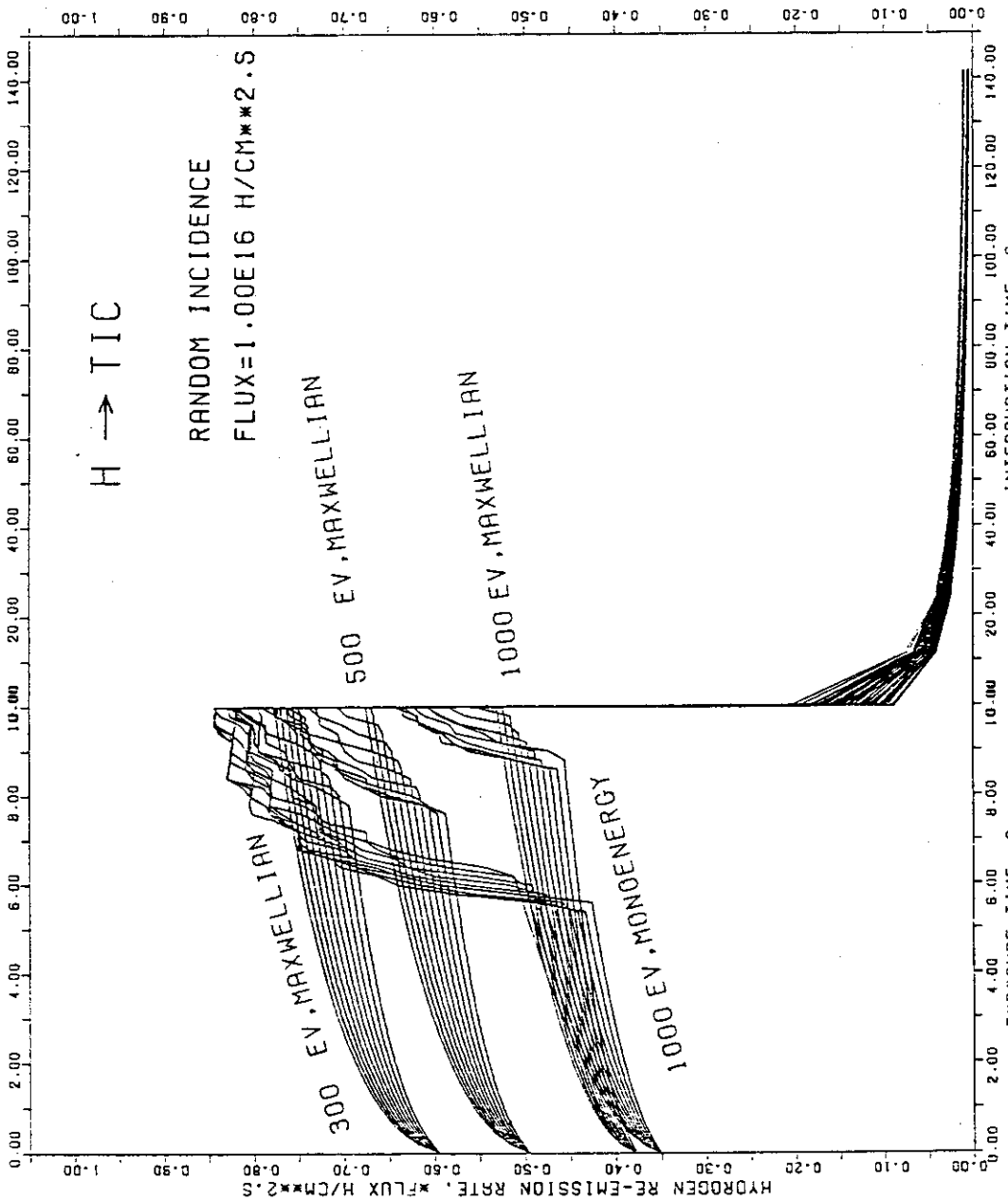

Fig. 6 Variation of recycling rate of hydrogen with shot number (up to the 10th shot) as a function of time in TiC for some different energies. Operation schedule of one shot: 10 sec discharge and 10 min interruption [29].